EXPERIMENTAL AND NUMERICAL INVESTIGATIONS ON FRACTURE CHARACTERISTICS OF 3D PRINTED MATERIAL BASED ON SIZE EFFECT LAW

By

Sumitkumar Yogeshbhai Patel

(Enrollment No: 179999919059)

Research Scholar, Gujarat Technological University

Supervised By

Dr. Chaitanya K. Desai

Professor,

MED, CKPCET, Surat,

A Synopsis Report Submitted to Gujarat Technological University
for the Award of Doctor of Philosophy
in Mechanical Engineering

April 2025

GUJARAT TECHNOLOGICAL UNIVERSITY, AHMEDABAD

EXPERIMENTAL AND NUMERICAL INVESTIGATIONS ON FRACTURE CHARACTERISTICS OF 3D PRINTED MATERIAL BASED ON SIZE EFFECT LAW

Submitted By
Sumitkumar Yogeshbhai Patel

Abstract

The use of 3D printed parts for building large structure requires the scaling of their mechanical properties. The main objective of this work to characterize, experimentally and numerically, the size effect of 3d Printed material. Fused deposition modeling (FDM) is one of the 3d Printing method used in this work. This study deals with three different thickness laminate made with FDM method. All laminate have same build raster angel but different sizes and layer thickness. Effect of thickness also studied on the size effect and fracture parameter. This study also deals with an experimental and numerical investigation on the efficacy of size effect testing to characterize the fracturing behaviour of specimens made using FDM method. Size effect method is easier to implement than other methods for measuring the fracture properties. Thickness effect on the size effect and fracture parameter also considered for investigation. Two types od specimen, Single edge notched tension(SENT) and double edge notched tension (DENT), assessed for size effect and fracture parameter. FE simulation on DENT and SENT specimens with the calibrated traction separation law used for crack propagation analysis.

Academicians and industrialists are currently embracing the use of latest manufacturing method. Additive manufacturing also known as 3d printing is constantly evolving with exciting new applications emerging across various domains. Among various additive manufacturing method fused deposition modeling (FDM) is widely used for manufacturing various parts. The use of FDM parts for building large structure requires the scaling of their mechanical properties. The main purpose of this study is to conduct an experiment to evaluate the size impact of FDM-made parts. Here FDM parts are also check for their behaviour based on ductility level.

if FDM parts are quasi-brittle then to to conduct an experiment to evaluate the size effect of FDM-made parts and if their behaviour is ductile then to essential work of fracture method to evaluate fracture parameter. Among various FDM materials, this study aimed to investigate the mechanical and fracture properties of FDM parts made from carbon powder-reinforced polylactic acid (CPLA) and Polycarbonate (PC).

FDM parts requires the study of size effect on their mechanical properties, this study is often overlooked in literature on FDM material. Measurement of the size on the nominal strength of notched Specimens of carbon PLA plastics are reported. The main objective of the present work is extract the fracture properties of carbon PLA material using the size effect law. Generally, it has been reported in the literature that the 3D printed material behaves in the similar manner of the composite materials. The size effect is predominated in composite material. Hence, it is believed that the same law may exist in the 3D printed material. To test the efficacy of this statement, various specimens with single edge notched specimens(SENT) and double edge notched specimens (DENT) geometries are prepared with thickness values of 0.7,1.4 and 2.1 mm. The length to width ratio for all the specimens is kept constant as 2.225 and width varies in a range of 1:2:3:4. Based on the recorded data the fracture toughness is determined for both the geometries and its variation with size is predicted. The results indicates that the CPLA FDM printed materials too show the size effect.

Numerical analysis Using Abaqus software also done and experimental and numerical results are compared. Numerical analysis of crack tip plastic zone also done using Matlab and crack initiation criteria discussed. Polycarbonate (PC) FDM material is also used in this work. Different specimens with varying raster angles were prepared and tested on a UTM. If the material behavior is quasi-brittle, then the SEL approach is applied; if ductile behavior is observed, then the essential work of fracture concept is applied. Here, material behavior is determined based on the ductility level approach.

Contents

List of Figures

Chapter 1

Synopsis of the thesis

1.1 Brief description on the state of the art of the research topic:

Engineering structures can fail due to various reasons, including uncertainties in the loading or environment, inadequacies in design, defects in the materials, and deficiencies in construction or maintenance. Generally disasters occur because engineering structures contain cracks-arising either during production or during service, and the consequences can be fatal. Catastrophes have been witnessed in wide ranges of applications involving aeronautics, automobiles, bridges and highways, and great loss has been induced in human life and economics

Defects in materials are inevitable, and complex factors are often involved in the scope of the entire picture. The principles of mechanics for continuous media break down when engineering structures contain cracks. Over the past fifty years, contributions have been made for the understanding of crack-related structural failures and various approaches were introduced to deal with the problems. Material science looks into the microscopic composition and crystallographic defects of materials and provides us with understandings about the fundamentals of crack nucleation and crack propagation. Fracture mechanics aims at studying the driving force on a macroscopic crack and the material's resistance to fracture.

Consider the two solid bodies Ω_1 and Ω_2 separated by a common interface in the initial configuration as shown in Fig. 1.1. Ω_1 and Ω_2 could also be two regions of the same body connected by a thin (localised) zone of different nature (yield zone or craze). If the body is subjected to prescribed tractions and if interface separates (fractures), then the separation process creates a pair of new surfaces violating the fundamental laws of continuity. The newly formed region cannot be uniquely mapped from the undeformed configuration. This is a fundamental problem in modeling fracture in the framework of the mechanics of continuous media.

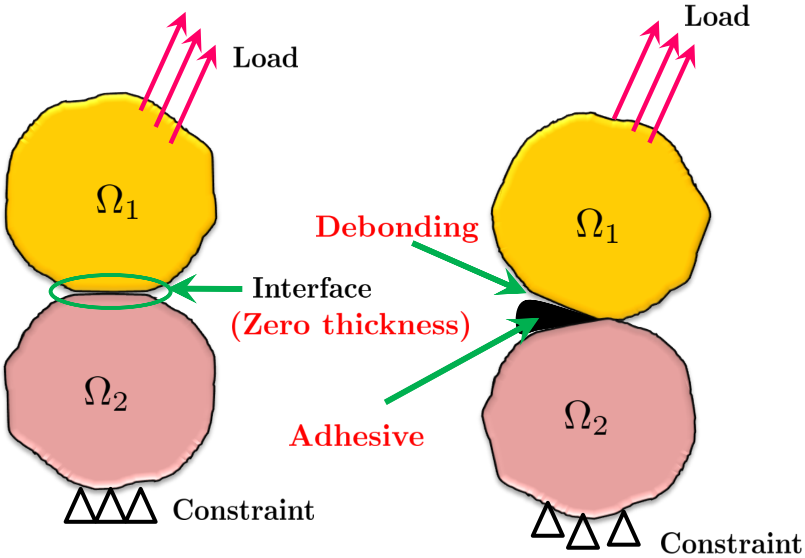

Figure 1.1: Schematic diagram of the interface and its debonding.

Fracture mechanics in general is used to understand and predict structural failure due to the presence of cracks, which could not be captured by classical theories of elasticity and plasticity. Damage models are based on the porous plasticity which describes the effects of nucleation, growth and coalescence of voids on the load bearing capacity of a material volume as a function of the local stresses acting on that volume. While the cohesive zone model (CZM) describes material failure on a phenomenological basis The advantage of this model when compared to LEFM is that the parameters of the model depend on the material and not on the geometry. This concept guarantees transferability from specimen to structure over a wide range of geometries. CZM approach is easy to implement in finite element analysis (FEA) compared to the other two approaches. In this work, parameter for CZM model are derived by the size effect law (SEL) and essential work of fracture (EWF) method, The SEL is applicable to the quasi-brittle material and EFW is applicable to ductile material.

Additive manufacturing (AM), more frequently recognized as one of the important 3D printing method or technique of rapidly developed the product, adding layer one over another, which also recognized as rapid prototyping (RP).

The first Rapid Prototyping technique was developed in the late 1980s and this technique were basically used for creating models and prototype parts. As the construction time is very fast, it was typically used for make model/prototype in the starting. This method itself is actually recognized with high expectations for the upcoming days to substitute some additional complex and outdated traditions of construction.

3D printing is a newly and very advanced AM technology which creates models or prototype which are already designed. High class prototype irrespective the intricacy of its geometry is also effortlessly produced by this technology without making any defect in less time period. In CAD software it is possible to meshed 3D computer model/prototype and it will be created by image data. After doing such process A STL file is commonly formed. The 3D printing material takes additional sliced data file of 2D layers [Wang et al. (2017)]]. For this process, STL data file is essential object for printing the part in 3d printer. This parts are first processed by a piece of slicing software which slice the model into layer by layer and generate a G-Code file which contains instructions for a particular printer. G-code commands are required to make each layer of raw material for the making of prototype which comes from series of cross sections. To create final shape of the model virtual c/s of the CAD model should be fused in proper way.

Components manufactured using 3D printing technology has various applications in automotive engineering (Talagani et al., 2015), aerospace industries (Kobryn et al., 2006; Murr, 2016), medical fields (Murr, 2016; Ji and Guvendiren, 2017) and architectural industries.The main problem in the application of such product which are manufactured by 3D printer is the mechanical properties of the product which dependences on too many building parameters. So, it is very important to study on all these parameters and the way these parameters are going to affect individually to the strength of the end product. Modern development of the 3-D printers are made them very easy to operate to the society at very low costs. Most of the low-cost printers are manufactured from ABS or polylactic acid PLA. The application point of view this technology has grown widely in the last era in scope as well as volume vise due to the accessibility of low-cost 3D-printing strategies. There are number of experimental rapid prototyping methodologies may be in development or it may be used by small groups of companies. RP techniques which are presently commercially available are Stereolithography (SLA), Selective Laser Sintering (SLS), Laminated Object Manufacturing (LOM), Fused Deposition Modeling (FDM), Solid Ground Curing (SGC) and Ink Jet printing techniques. [Raut et al. (2014)]. FDM techniques convert material into liquid to make layers, SLS technique makes solid mass of material into powder form using laser and in stereolithography technique cure liquid material using photo solidification. Solidification any kind of reaction are usually chain growth polymerization which occurs only in light showing region. Among all these techniques of RP, Fused Deposition Modeling is broadly used in industry[Mohamed et al. (2016)]].

1.2 Fused deposition modeling (FDM)

In 1990s, Stratasys Inc. introduced the FDM process as a concept modeling [Mohamed et al. (2016)]. FDM technique is recognized for easy use for house hold purpose. It can be transformed in to desktop 3D printing. It is to be noted that FDM prints components into one layer over another and all the layers are arranged in a way of line drawing. There are various technique like, ink-jet printing, gravure and flexography for that FDM technique can be considered as one of alternative to adjust various kind of textile substrate [Garg and Bhattacharya (2017)]. Now a days, FDM becomes very useful tool for the production of fixture and various other functional parts. As the application area increase, FDM requires various specifications with respect to geometrical characterization.

In FDM, any complicated solid component is created due to one layer over another and it starts from bottom side. Every layer can be deposited on current surface otherwise printing material having problem that it will hardens in the air. Boundary should be finite for projection of material over another material. Boundary can be enlarged as the material cools down at very faster rate. This technology is widely used for prototyping and manufacturing application. Without any tooling FDM makes 3D geometries. [Mohamed et al. (2016)]. Figure 1.2 shows the schematic diagram of FDM technique. This technology began as a process for creating prototype parts; recently it has found new usefulness in the production of manufacturing tools and as a manufacturing process for end-use parts. In order to be used as a part for serial production, the components must possess the required mechanical properties [Raut et al. (2014)]]. For developing of 3D compound components, FDM becomes one of the best technique in which material formed one layer over another in X and Y direction through very precisely working of liquefier nozzle. As the platform is created by material layer it will move towards Z direction and another layer is introduced. Fused deposition modeling(FDM) technique deposits a molten filament of ABS in a criss-cross manner resulting in direction dependent, or anisotropic, material properties [Garg and Bhattacharya (2017)]. In FDM process, particularly second number nozzle extrudes support material that provide support to the structure as well as it has an overhang angle 45° by default. If this overhang angle is less than 45° there may be chances of falling of bead. Vertical extruder is used for melting thermoplastic material and it deposits on the horizontal axis platform. After some time it cools and converted into solid. In this process, extruder and the platform having controlled relative motion with respect to horizontal plane. As the first process of layer is complete in next process platform moves in downward vertical direction to facilitate next layer built up to weld together. Using the appropriate programming software it is possible to create extrusion trajectories. As per the fabrication procedure, i.e. manufacturing layer by layer, as described in Figure 1.2.

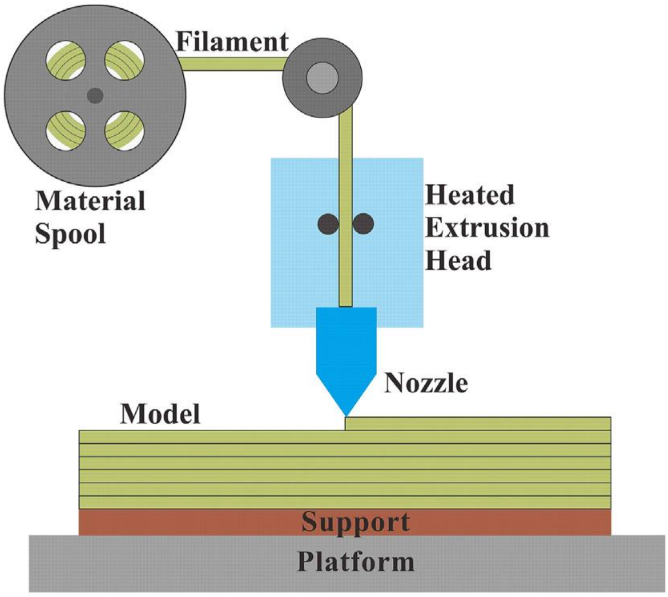

Figure 1.2: Schematic view of model is built layer by layer

In 3D printing technique/process property of printed material is the most important aspect. There are numerous process parameters that are directly or indirectly affect the 3D printed material properties through distortion of manufacturing object, configuration of mesostructure Throughout the FDM process. There are various parameters to be consider which affects the performance of the process, such parameter are layer thickness, air gap,pattern, raster angle etc. The influence of this parameter is to be checked by various mechanical testing methods like, compression, tension, bending [Zou et al. (2016)]. This parameter affect Strength, roughness and geometric accuracy of the final fabricated parts [Garg and Bhattacharya (2017)]. In FDM process, raster fill is one the important process tool that fills the part layer [Bagsik and Manufacturing (2011)]. Raster angle is the angle between the path of the nozzle X -axis of the printing bed.The layers are differing by 90 degree among two layers. The starting accuracy and mechanical performance are affected by this angle and it can be designated from 0 to 90 degree [Wu et al. (2017). The stiffness and tensile strength will increase due to negative air gap. It is proven from experimental results that five process parameters, among all air gap and raster orientation had significant effects on tensile strength as related to processing temperature raster width and filament color[Zou et al. (2016)].

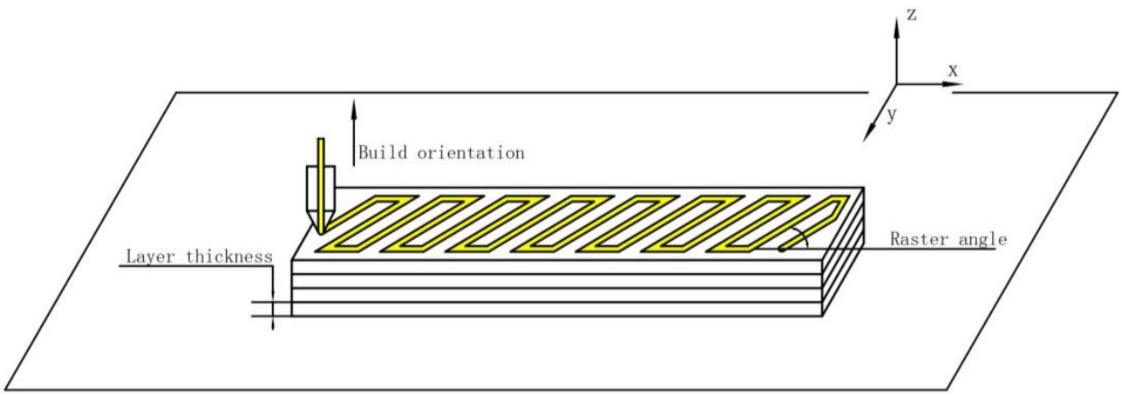

Figure 1.3: Schematic Thickness of layer, raster angle and building orientation in 3D model

As the mechanical properties of the end product are too sensitive, the minor change in process parameters, changes it melodramatically and this properties of parent material are very low compared to end product. Layer thickness is one of the important parameters that affect the properties mechanically which can be defined as the thickness of each layer come from nozzle. Due to accumulation of material layer one over another, the accuracy of printed samples down and thickness of layer and surface roughness rises. The accuracy of printed sample increase as layer thickness decreases. Similarly, rise in printing time is also going to increase accuracy of final product. Molding accuracy, nozzle diameter and material properties affected by choice of layer thickness [Wu et al. (2017)]. In FDM process, to create new part number of parameters is to be transformed[Bagsik and Manufacturing (2011)].

1.3 Size Effect Law

Failure of any material can be explained by taking relationship between stress and strain. Relation between stress and strain are given by different failure criteria. The basic failure criteria are maximum stress, maximum strain, deviatoric strain energy and the tensor polynomial criteria. These criteria does not involves micro mechanical failure which occurs mostly near the notches because these criteria are macro mechanical. But when the failure criteria involves energy than the whole scenario is going to be change. The most important consequence for that is **"Size Effect"**. From the classical theories of elastic materials and plastic materials, every structure made from the same material has a nominal strength which is not dependent on the Size of the structure.The Size effect caused by fracture energy release, this comes to a picture in the studies of concrete, rocks, ceramic and other quasi brittle material. It has been found that the size effect is transitional between plasticity and linear elastic fracture mechanics(for LEFM,Size effect is prominent). However, due to orthotropic nature, fracture behavior of components made of FDM process play critical role while using in large structure, In these components during fracture, a large non-linear fracture process zone (FPZ) is observed where micro cracks initiates, grow and eventually coalesce to a crack. The strength and stability of the components can be predicted well provided th size of the FPZ is known. One of the approach to predict the geometrical parameters of FPZ is size effect law (SEL), which is defined by comparing the nominal strength (nominal stress at failure) σ_n of geometrically similar structures of different sizes. The size effect, proposed by(Bazant and Planas, 1998), is understood as the dependence of σ_n on the structure size D (characteristic dimension). According to the plastic limit analysis, as well as any theory in which the material failure is characterized in terms of stresses or strains, σ_n is independent of the structural size, i.e. there is no size effect. In linear elastic fracture mechanics, in which all the fracture process is assumed to occur at a point - the crack tip - σ_n declines in proportion to $D^{-1/2}$. This means that the plot of $\log(\sigma_n)$ versus $\log(D)$ (see figure 1.4) is an inclined straight line of slope $-1/2$, provided that the cracks at the moment of failure of structures of different sizes are geometrically similar. The size effect caused by fracture energy release has recently come to the attention in studies of quasi brittle materials like concrete, composites, natural composites etc. Note that the similarity of cracks at failure has been experimentally demonstrated for most, though not all, types of failures of concrete structures of different sizes, in the usual size range. No such information is available for FDM structures.

The measurement of constitutive properties and dimensions of FPZ in FDM parts have not been reported and still an active area of research in the field of AM. Furthure to check the efficacy of the experimentally extracted constitutive properties of FPZ, these parameters are then used for numerical simulation to predict the global response. Cohesive zone model (CZM) concept is widely used to study a wide variety of physical phenomena for example crack growth along a prescribed plane in elastic-plastic material (Li and Chandra, 2003; Shet and Chandra, 2002; Hui et al., 1992), failure of adhesive joint (Pardoen et al., 2005; Zhu et al., 2009) and fiber bridging and debonding in composite material (Li et al., 2005). The concept of CZM was proposed by Dugdale (1960) andG.I. (1959). In CZM, the FPZ is regarded a cohesive zone which are connected by cohesive traction and separates during deformation. The idea is to capture the complex deformation behaviour in FPZ using simple CZM for crack propagation

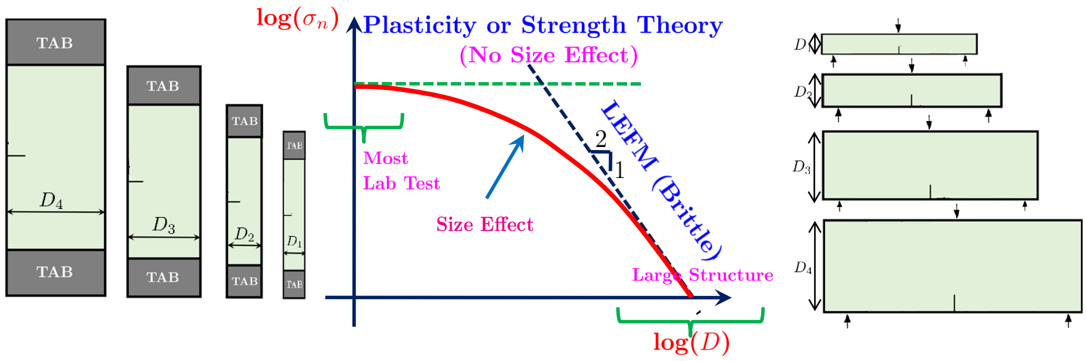

Figure 1.4: Concept of size effect

analysis. The relation between cohesive traction and displacement jump of cohesive surface is usually called the traction separation law (TSL) in CZM while the area under TSL describes the energy release rate. The shape of the traction separation curve and the value of cohesive parameters are the key features of CZM. Many variation of CZM have been and successfully applied to predict fracture behaviours. Needleman (1987) first proposed a polynomial law for describing the process of void nucleation in metal matrices. Needleman (1990a) further used the exponential models to study crack growth in brittle material under dynamic loading condition. Tvergaard and Hutchinson (1992) use a trapezoidal traction separation model to evaluate the crack growth resistance in elasto plastic material. Suresh (1983) adopted a linear cohesive law for interganuler fracture behavoiur. Applications of the CZM mostly fall in the range of exponential, linear/bilinear, polynomial, trapezoidal and tabular forms of traction-separation laws. Desai et al. (2016) have used CZM to simulate failure in adhesive joints. They used traction separation law obtained iteratively by matching the numerical load-displacement data to that obtained in experiments. The main objective of the present study is to extract the parameters and shape of TSL for carbon/PLA material made of FDM. Martinez AB et al. Martinez AB (2009) proposed another approach by defining the ductility level. Attention was given to the accurate determination of the lower L threshold separating the mixed. mode state from the plane stress one. They have proposed ductility level $(D_L) = d_r/l$ for nothced specimen, where d_r is displacement at rupture and l is ligament length. When the average ductility levels are compared with the different fracture types it can be appreciated a correspondence. If D_L is less than 0.15, then quasi-brittle behavior is observed and the SEL method can be applied. If D_L is greater than 0.15, then ductile behavior is observed and the EWF approach can be applied.

1.4 Definition of the Problem

Extensive research has been conducted to determine the mechanical characteristics and the impact of process parameters of FDM partsPanneerselvam et al. (2021); Maszybrocka et al. (2022); Rouf et al. (2022); Sagias et al. (2018); Ai and Vogt (2022).To extract fracture property of FDM printed parts is still scope for further research. Therefore,the current study aims to investigate the fracture properties and SEL of FDM parts behaves as quasi brittle material with varying thickness, following the approach by Bazant et al(Bazant and Planas, 1998). Cohesive zone model concept is widely used for crack propagation analysis in various material systems when subjected to different loadings. For effective use of CZM, its parameters like maximum traction, critical separation, cohesive energy and most importantly its shape needs to be calibrated experimentally. Study also includes to use SEL to extract the CZM parameters and used those parameter for FEA. The literature suggests that there have been relatively few literature is reported at FEA of FDM parts. So here the dog bone and fracture specimens have been prepared using FDM process. If FDM parts shows quasi-brittle behaviour then SEL method to be applied using changing layer thickness and geometry of specimen. If FDM parts shows ductile behaviour then the EWF approach will be applied for study fracture property using varying raster angle. Material behaviour will identified based on ductility level.

1.5 Objectives and scope of work

1.5.1 Objectives

Objectives of the current study are focused on the development and characterization of parts made with Fused deposition Modeling method , as well as investigating their mechanical and fracture properties. Based on this, objectives are listed below:

- The objective of this work is to manufacture specimens with various geometries, sizes, raster angles and thicknesses using the FDM method. Carbon powder reinforced polylactic acid (CPLA) and Polycarbonate (PC) filaments are used to manufactured FDM parts.
- If the material is behaving like a quasi brittle than objective is to find the size dependence of material because quasi brittle is size dependent.
- To determine the fracture energy and length of the fracture process zone using the size effect law for specimens with different thicknesses and raster

orientations.

- To determine the cohesive zone model parameters of FDM manufactured specimens using Size effect law and EWF method
- To test the efficacy of the experimentally measured CZM parameter using finite element simulation (FEM) by comparing local as well as global response.
- If the material is not quasi-brittle, other methods for determining fracture energy will be discussed
- To study various factor affecting the parameter of CZM and SEL. various parameter such as Specimen geometry, Material, Thickness of Specimen, symmetric effect, size effect and EWF method for FDM manufactured specimens.

1.5.2 Scope for research

The current study aims to investigate the mechanical properties, size effects, and fracture properties of FDM parts of varying layer height, raster angle and thickness. The study intends to analyse the size effect on the nominal strength of FDM parts within the framework of Bazant's size effect law. By conducting experiments and potentially incorporating theoretical analysis, this research aims to contribute to the understanding of size effects and fracture behavior in FDM parts. Derived SEL parameter used for FEM to study crack propagation analysis. If behaviour of FDM parts found to be ductile then to apply EWF approach to derive TSC curve.

1.6 Original contribution by the thesis

In present work all specimens are manufactured by FDM method using CPLA and PC filament. Material behaviour is asses using ductility . If quasi-brittle material behaviour is found then SEL method given by (Bazant and Planas, 1998) is applied and ductile behaviour is found then EWF method is applied for fracture analysis of FDM parts. To assess the mechanical properties of the FDM parts, an in-plane tension test was conducted following the guidelines of ASTM D638-14. Also, the statistical analysis of FDM parts has been performed to determine tensile strength at different orientations using a regression model. To extract fracture properties, three sets of Single edge notched tension (SENT) and double edge notched tension (DENT) specimens were prepared using CPLA filament. The SENT and DENT specimens were fabricated from laminates with orientations of $[\pm 45/0]_s$ raster angles, at different thicknesses of (in mm) of 0.7 , 1.4 and 2.1.The fracture test of SENT and DENT specimens aimed to investigate the effect of specimen size (width, D) on the nominal strength (σ_n) of the FDM prats for all sets. The results showed that the nominal strength depended on the specimen size, and this relationship was analyzed. Based on the experimental data, size effect curves were plotted, and it was observed that they followed Bažant's size effect law. This law describes the relationship between specimen size and nominal strength. Using the size effect law, the fracture energy (G_f) and the effective length of the fracture progress zone (C_f) were calculated. Additionally, the cohesive energy was determined using the traction separation law The traction separation curve (TSC) obtained from the size effect law which is used in finite element analysis of SENT and DENT specimens for crack propagation analysis using cohesive zone modeling (CZM) technique. For PC filament made FDM parts ductile behavior is found so the EWF method is applied for different raster angle orientation specimens. For EWF approach DENT specimens with different rater angle were prepared using FDM method. Each raster angle specimen sets consist of different ligament length specimen which were tested on UTM machine. Then EWF methods were applied on tested specimen to calculate fracture energy.

1.7 Methodology of Research and Result and discussion

1.7.1 Methodology of Research

1. Selection of 3d filament material and preparation of specimen using FDM methodology.

2. Dog-bone Specimens' preparation to extract material characteristics as per ASTM D638-14.

3. For deriving the SEL, fracture specimens were prepared using single edge notched tension (SENT) and double edge notched tension (DENT) specimens of thickness 0.7 mm, 1.4 mm and 2.1 mm. All the specimens were made of six layers with raster orientation of $[\pm 45/0]_s$ with layer thickness(h) of 0.12 mm, 0.23 mm and 0.35 mm respectively. Four different geometrical dimensions, with constant L/D ratio, were selected with scaling factors 1:2:3:4 as proposed by Basant (Bazant and Planas (1998); Bazant et al. (1996)) Details are shown in table 1.1, 1.2, figure 1.5 and figure 1.6

4. Testing of the specimen on the tensile testing machine to extract load-displacement data.

Table 1.1: Dimensions of the SENT specimens.(mm)

Size	Width(D)	Gauge length,L	Length	Crack Length(a)	Thickness
1	7.5	16.69	92.69	1.5	0.7 1.4 2.1
2	15	33.39	109.38	3	0.7 1.4 2.1
3	22.5	50.06	126.06	4.5	0.7 1.4 2.1
4	30	66.75	142.75	6.0	0.7 1.4 2.1

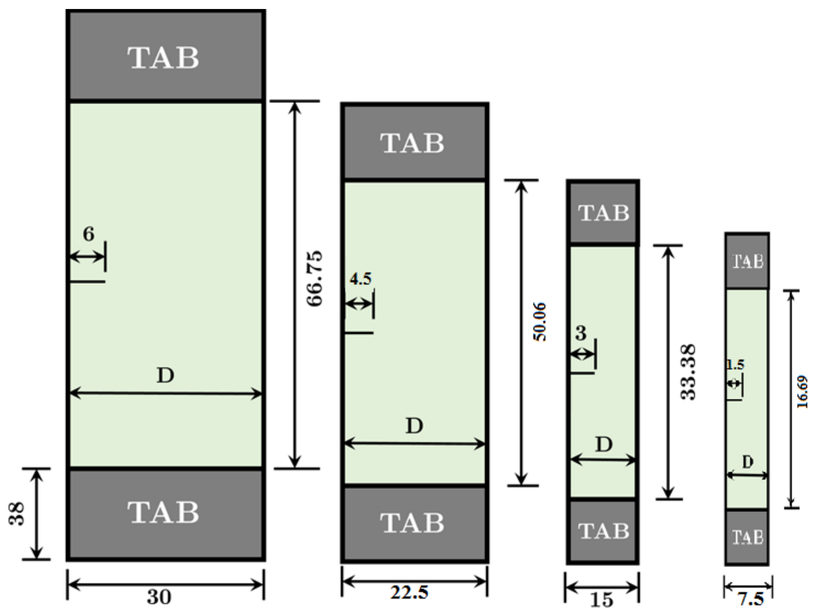

Figure 1.5: Schematic of SENT Specimen

5. If quasi brittle behaviour is found based on ductility level then apply size effect law from experimental data using regression analysis. Extract fracture properties from Size effect law.

Table 1.2: Dimensions of the DENT specimens.

Size	Width(D)	Gauge length,L	Length	Crack Length(a)	Thickness
1	7.5	16.69	92.69	0.468	0.7 1.4 2.1
2	15	33.39	109.38	0.937	0.7 1.4 2.1
3	22.5	50.06	126.06	1.4	0.7 1.4 2.1
4	30	66.75	142.75	1.1875	0.7 1.4 2.1

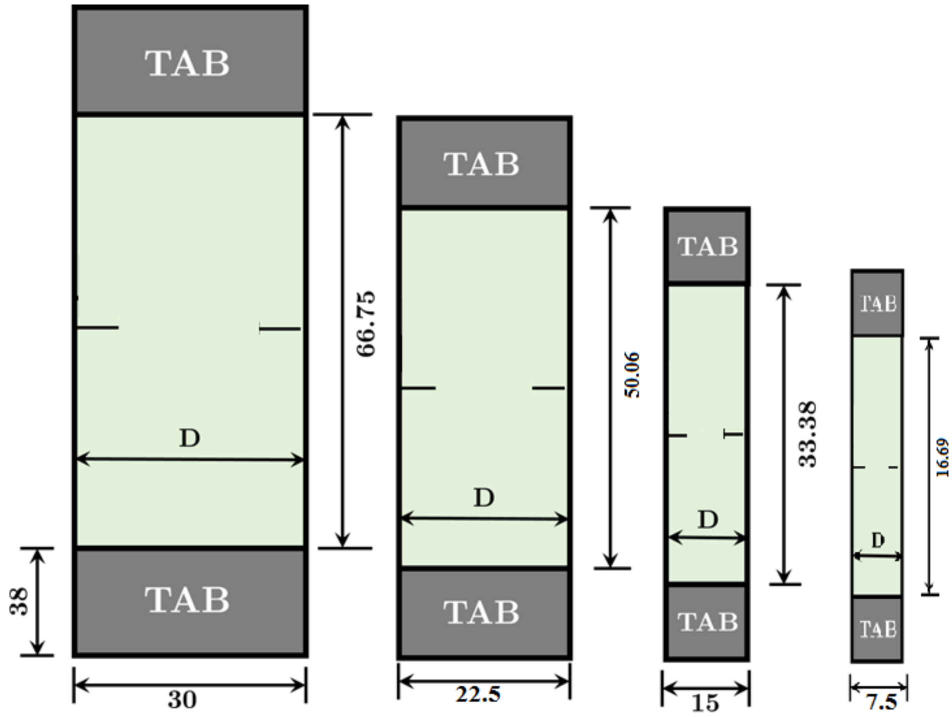

Figure 1.6: Schematic of DENT Specimen

1.8 Result and Discussion

Experiments on FDM-made parts were conducted to analyze their material behavior, as outlined below

a Tensile strength analysis :The tensile strength of CPLA and PC material FDM parts was measured using a Tinius Olsen/l-series H50kL Universal Testing Machine (UTM)

b Size Effect Law and Fracture Properties Analysis : This section presents a mathematical analysis of the size effect law, employing experimental data and regression analysis fro quasi brittle FDM material. The size effect law was used to determine the fracture properties of the materials. Subsequently, a derived TSC was incorporated into a Finite Element Method (FEM) analysis to study crack propagation and evaluate the efficacy of the derived TSC

c Essential work of fracture analysis : This section presents an implementation of the EWF concept to FDM parts exhibiting ductile behavior. Fracture parameters are then derived using the EWF method

1.9 Tensile strength analysis

For the present work, mechanical properties of carbon PLA filament with 20% carbon powder and 80% PLA were measured using a dogbone shaped test specimen according to ASTM D638-14 (see Figure 1.7)(ASTM). All specimens were prepared with a thickness(t) of 1.4 mm using FDM process with raster angles(θ) of 0, 45 and 90. The printing parameters such as bed temperature(60°), nozzle temperature(220°), printing speed (20 mm/s), and infill density (100%) were kept constant during specimen preparation. For each raster angle, three different layer thicknesses(h), 0.12 mm, 0.23 mm and 0.35 mm were selected to build final 1.4 mm thickness of the specimen. Five specimens for each raster angles were tested at room temperature with constant crosshead speed of 5 mm/min. All the testes were performed using UTM. The results of stress-stress curves are shown in Fig. **??** for all cases reported. From the results the elastic modulus in longitudinal direction (E_1), transverse direction (E_2) and modulus for raster angle 45° (E_{45}) were measured. The shear modulus(G_{12}) was calculated using relation $G_{12} = 1/(\frac{4}{E_{45}} - \frac{1}{E_1} - \frac{1}{E_2} + \frac{2\mu_{12}}{E_1})$ proposed by Zhao et al. (2019). The results are reported in table 1.4 for all cases. The classical laminated theory (CLT) of theory Casavola et al. (2016) applied for calculation elastic modulus of $[\pm 45/0]_s$ raster orientation specimens and presented in table 1.4.

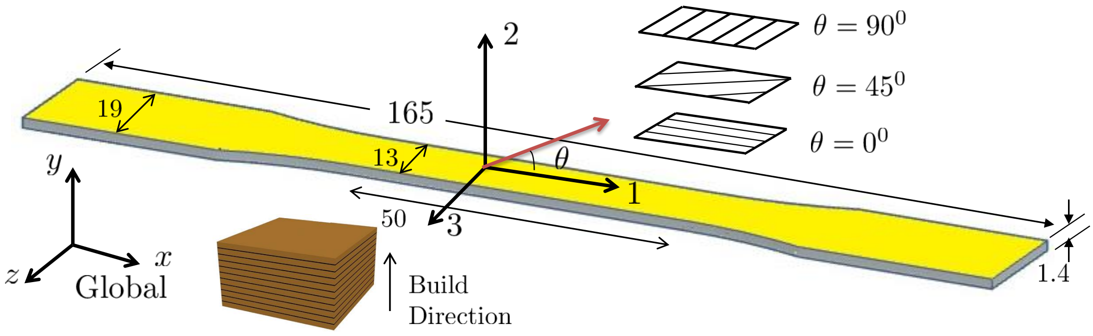

Figure 1.7: ASTM D638 Shape of specimen with Details.[ASTM]

Table 1.3: Mechanical test data for the FDM AM Carbon PLA

Layer thickness (mm)	E_1 (MPa)	E_{45} (MPa)	E_2 (MPa)	ν_{12}	G_{12} (MPa)
0.35	1980	1561	980	0.36	713.96
0.23	2085	1642	1028	0.36	752.44
0.12	2189	1730	1057	0.36	807.7

Table 1.4: Mechanical property for the FDM CPLA Laminate using CLT

Layer thick. (mm)	E_x Exp. (MPa)	E_x (MPa)	E_y (MPa)	E_z (MPa)	ν_{xy}	ν_{xz}	ν_{yz}	G_{xy} (MPa)	G_{xz} (MPa)	G_{yz} (MPa)
0.35	1760	1772	1427	1427	0.20	0.20	0.4	639	639	509
0.23		1865	1502	1502	0.20	0.20	0.4	673	673	536
0.12		1970	1579	1579	0.19	0.19	0.38	711	711	572

1.9.1 Size Effect Law and Fracture Properties Analysis

For deriving the SEL, fracture tests were conducted using single edge notched tension (SENT) and double edge notched tension (DENT) specimens as mentions in methodology section. These specimens were tested on UTM under constant cross head displacement of 2 mm/min (see fig **??**). Initial crack was put using laser cutting machine (crack tip radius was 0.2 mm measured from video images). The crack length in SENT and DENT specimens were selected as $D/5$ and $D/16$ respectively (Bazant et al. (1996)). To further ensure that the failure must initiates from the crack tip, the gripping length was selected as 38 mm at both ends. All the tests were performed at room temperature and rate effects were neglected. During the experiments, load and displacement data were recorded which were further used to predict the SEL. After the completion of the experiments, Load(P) - Displacement(Δ) data were analyze. Fig. 1.8 and Fig. 1.9 shows the $P - \Delta$ curves

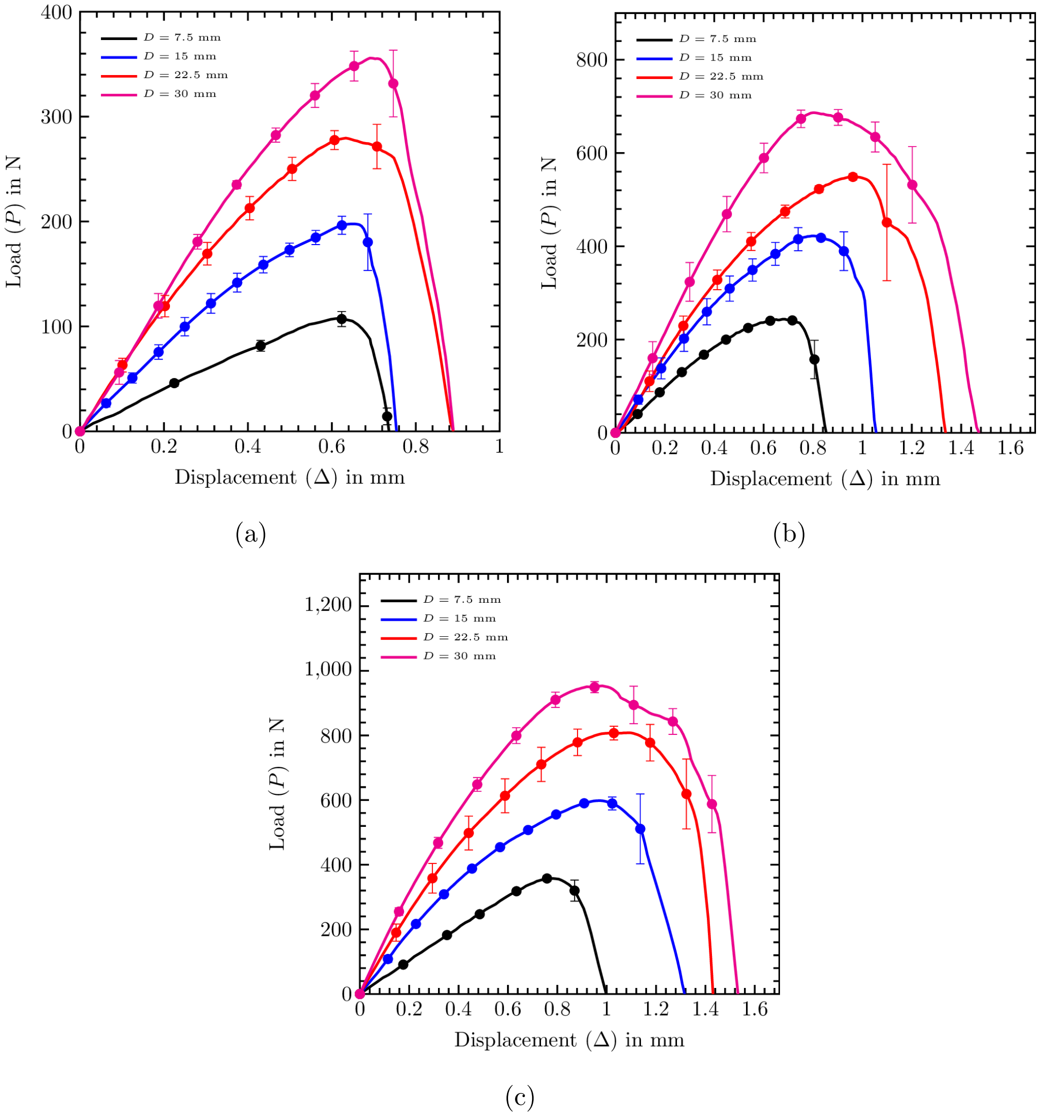

Figure 1.8: Load-displacement diagram of SENT Specimens (a)t = 0.7 mm (b) t = 1.4 mm (c) t = 2.1 mm

for the various sizes and thickness specimens. For the each geometry four specimen tested and result displayed with error bar as shown in Fig. 1.8 and Fig. 1.9. Error bar data plotted at specific interval for clarity in Figure.

These curves indicate that they are almost linear up to failure. This failure is a clear indication of pronounced brittle behavior of material. In opposite to that non linear section after peak load indicates inelastic behavior of material. As a effect, the failures were catastrophic and occurred shortly after the peak load. Failure consisting of delamination between layer and micro cracks in layer in layers was observed in the experiments. Experimental test results are summarized in Table 1.5. The specimen nominal strength (σ_N) in table defined as the average stress at failure based on the unnotched cross section of specimen, $\sigma_N = P_{max}/Dt$ where

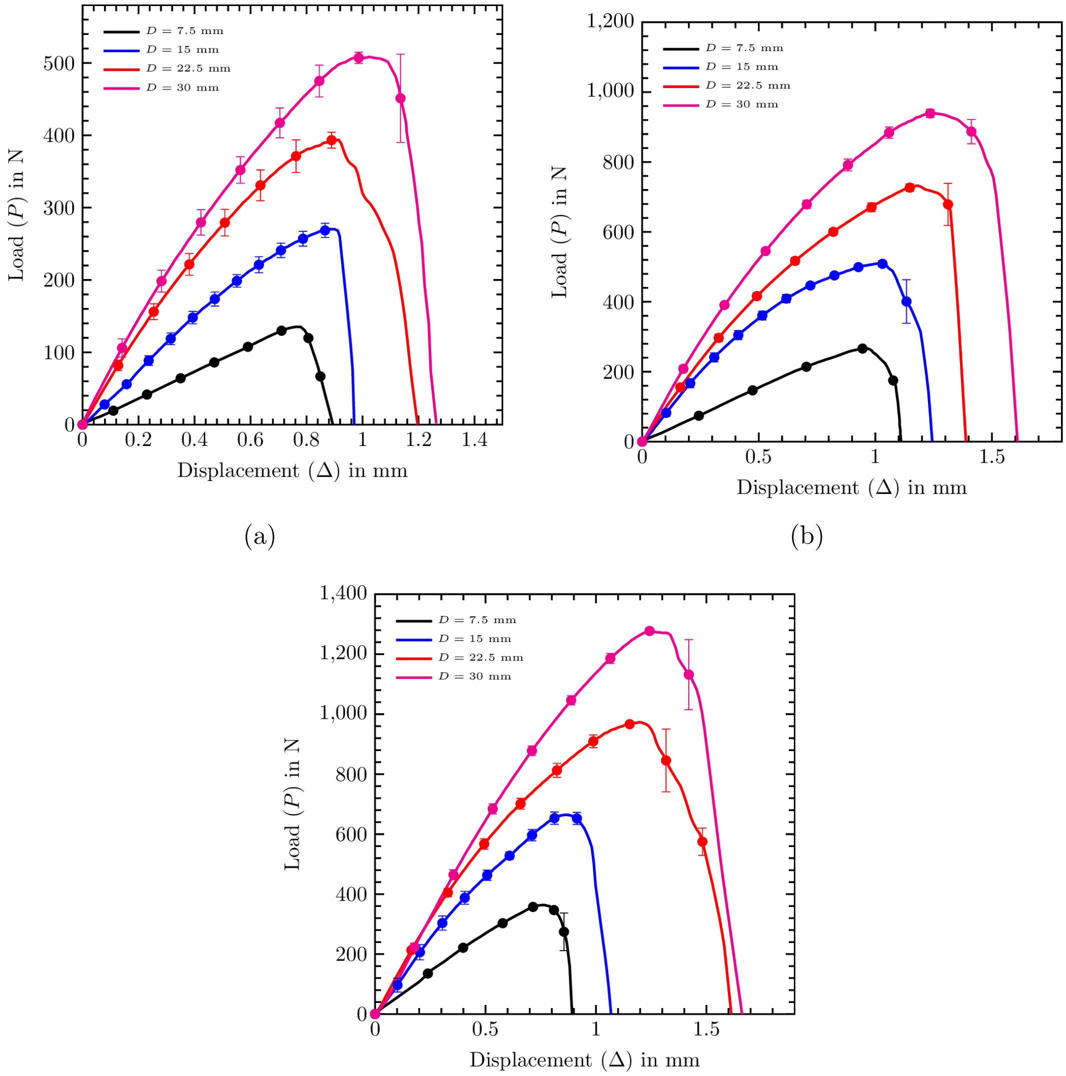

(a) (b) (c)

Figure 1.9: Load-displacement diagram of DENT Specimens (a)t = 0.7 mm (b) t = 1.4 mm (c) t = 2.1 mm

t is thickness of specimen. Average nominal strength is reported in table as four specimens tested for the each geometry.

Structure which have notched pre-exits can be analyzed by size effect of Type-II (Bazant and Planas, 1998; Bažant et al., 1993; Bazant, 1984). Type-II size effect relates the nominal strength (σ_N) to the characteristics size of structure(D). Size effect law parameters were determined by regression analysis of experimental data. Following Bazant (1984), for quasi brittle structures the size effect of type-II given by

$$\sigma_N = \sigma_0 \left(1 + \frac{D}{D_0}\right)^{-\frac{1}{2}} \tag{1.1}$$

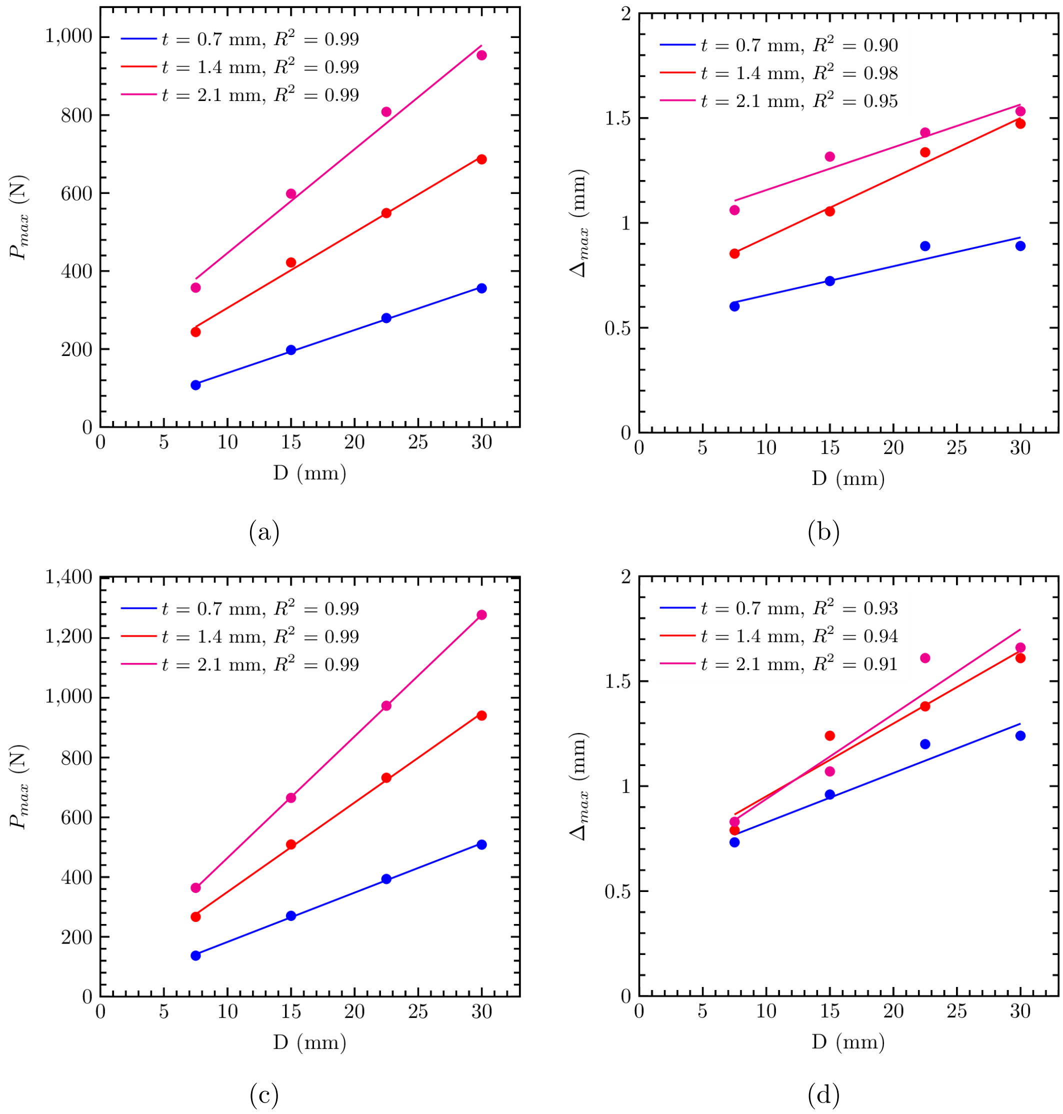

Figure 1.10: Maximum load- size of specimen for (a) SENT (c) DENT and Displacement at failure -size of Specimen for (b) SENT (d) DENT

where $\sigma_N = C_n P_{max}/Dt$ = nominal strength, C_N= chosen coefficient introduced for convenience, σ_0 and D_0 = constant depending on both fracture process zone and specimen geometry. The size effect law in (1.1) is expressed in the form

$$Y = C + AX \text{ where, } X = D, Y = \sigma_N^{-2} \text{ and } D_0 = \frac{C}{A} = \frac{\sigma_0^{-2}}{A} \tag{1.2}$$

A linear regression analysis was conducted by plotting Y versus X as shown in Fig.1.11a using experimental data of σ_N for specific size D of SENT geometry having 0.7 mm thickness. Similar analysis have been done for other thickness and DENT specimens The parameter of the size effect law were obtained from the slope and the vertical intercept of these plots. Same procedure were followed for SENT and DENT geometry of 0.7 mm, 1,4 mm and 2.1 mm thickness specimens.

Table 1.5: Result of Fracture Tensile Test on SENT and DENT Specimens

Specimen	Width (D) (mm)	σ_N (MPa) t =0.7 (mm)	t = 1.4(mm)	t=2.1(mm)
SENT	7.5	21.05	22.99	22.92
	15	19.36	20.54	19.04
	22.5	18.2	17.48	17.55
	30	17.02	16.36	15.24
DENT	7.5	26.99	25.5	23.17
	15	26.31	24.28	21.59
	22.5	25.38	23.51	20.61
	30	25.00	22.5	20.49

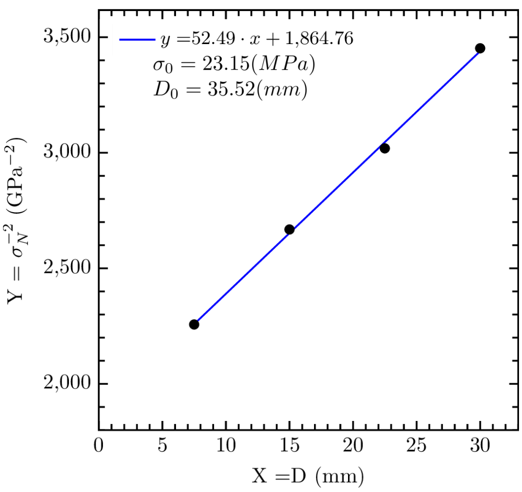

(a)

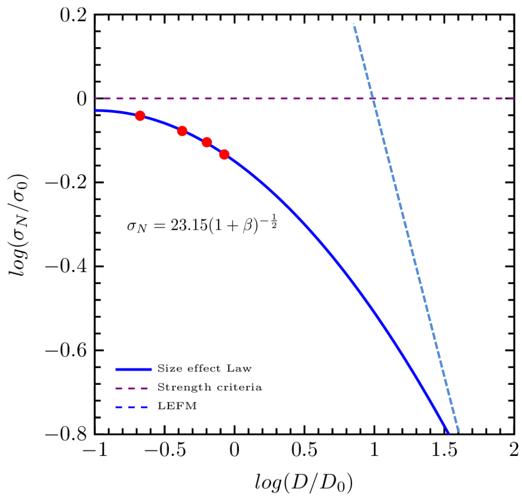

(b)

Figure 1.11: Regression analysis for (a) finding size effect parameter and (b) Obtained Size effect law for SENT 0.7 mm Specimens

The size effect law (SEL) parameter are shown in Table **??**. Size effect law can be obtained by plotting the normalized strength (σ_N/σ_0) as a function of the normalized characteristic size (D/D_0) in logarithmic scale and then polynomial fitting the curve which is as shown in Fig.1.11b. In SEL $\beta = D/D_0$. Same procedure were followed for all specimens and obtained results are shown in Table 1.6.

The Fig.1.11b shows how the material is going to change its behavior from strength criteria to LEFM means 0 slope to -0.5 slope. Representation of SEL in Fig.1.11b clearly showing that (1) failure of FDM carbon PLA material showing remarkable size effect and (2) this effect shows a gradual movement with increment of size from maximum strength criteria to LEFM. These results can be used for

Table 1.6: Size Effect Parameter for SENT and DENT

t (mm)	Specimen	D_0 (mm)	σ_0 (MPa)	Size effect law
0.7		35.52	23.15	$\sigma_N = 23.15(1+\beta)^{-\frac{1}{2}}$
1.4	SENT	14.09	28.75	$\sigma_N = 28.75(1+\beta)^{-\frac{1}{2}}$
2.1		11.01	29.74	$\sigma_N = 29.74(1+\beta)^{-\frac{1}{2}}$
0.7		123.02	27.78	$\sigma_N = 27.78(1+\beta)^{-\frac{1}{2}}$
1.4	DENT	73.58	26.74	$\sigma_N = 26.74(1+\beta)^{-\frac{1}{2}}$
2.1		74	23.94	$\sigma_N = 23.89(1+\beta)^{-\frac{1}{2}}$

Table 1.7: Fracture Properties of SENT and DENT obtained by size effect law

thickness(t) in mm	SENT		DENT	
	G_f in kJ/m^2	c_f in mm	G_f in kJ/m^2	c_f in mm
0.7	11.4	4.213	11.9	7.6458
1.4	7.73	1.6710	6.96	4.5733
2.1	6.49	1.306	5.91	4.6036

designing a any structure or for checking safety where crack can grow in a steady manner before failure. So, these results are important to extrapolate the data from testing of prototype to the big size structural parts. From the results obtained for size effect, It shows that SEL also depends on the thickness of the specimen. The SEL is changing significantly by changing thickness of specimen. The SEL has significant effect on specimen geometry (SENT and DENT) because of different crack length. Bao et al. (1992) have solved the energy release rate and the stress intensity factor for orthotropic specimens. Following Bazant and Planas (1998); Bazant (1984), they have derived the equations

$$G_f = \frac{\sigma_0^2}{E^*} D_0 g(\alpha_0), c_f = \frac{g(\alpha_0)}{g'(\alpha_0)} D_0 \tag{1.3}$$

where G_f = fracture energy of the material and c_f= effective fracture process zone(FPZ) length.

$$G_f = \frac{\sigma_0^2}{E^*} D_0 g(\alpha_0), c_f = \frac{g(\alpha_0)}{g'(\alpha_0)} D_0 \tag{1.4}$$

Using the value of σ_0 and D_0 from table **??**, value of G_f and c_f were calculated using eq. (1.4) and shown in table 1.7 Form the table 1.7, it has been observed that value of G_f for SENT and DENT specimen are almost same for respective thickness. This indicate s the geometry independent of fracture energy for respective thickness. Value of c_f is also showing same trend of decreasing with increasing in thickness. For SENT and DENT, value of c_f is different because c_f depends upon the initial crack length which is different for both geometry. By doing 3^{rd} order

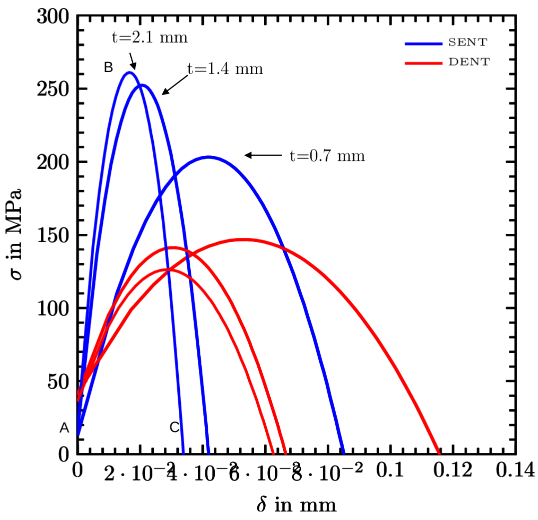

Figure 1.12: Traction-separation Curve

polynomial fitting of curve one can extract the traction-separation curve(TSC) for both SENT and DENT. Traction-separation curve can be used as cohesive element properties in FEM analysis of cracked specimens. This properties can easily extract from size effect law and shown in fig.1.12. It shows that maximum stress obtained by SENT specimens is at smaller opening compared to DENT specimens. It also indicate that though the size and shape of the traction-separation law for SENT and DENT are different but the fracture energy which is the area under the traction separation curve was constant so it treated as a material property. To study crack growth of FDM printed specimens underline the need for conducting numerical simulations to test the validity of the methods. A cohesive zone model can be used to simulate crack propagation analysis. Here strategy adopted where the traction separation curve is determined by size effect law. from that TSC is shown in fig.1.12.For simulation the 2D FE model consisted of three zones (a) Rigid zone(b) Carbon PLA laminate(Bulk material) (c) Cohesive zone for both DENT and SENT specimens have modeled in Abaqus standard finite element software Gripping section is assigned to be a rigid zone. Engineering constant material model derived form classical laminate theory is used for carbon pla laminate section. Crack propagation direction zone assign as a cohesive zone with damage for traction-separation law. This traction separation law is the same as that shown in fig.1.12 for each specimen type and thickness. Typical FE mesh in Abaqus standard constructed for each specimen type and thickness with CPS4R plane stress element in rigid & carbon pla laminate zone and COH2D4 cohesive element in cohesive zone Fig.1.13 compare experimental and numerical overall $P-\Delta$ response of the DENT and SENT specimens. Comparison is shown for specimens

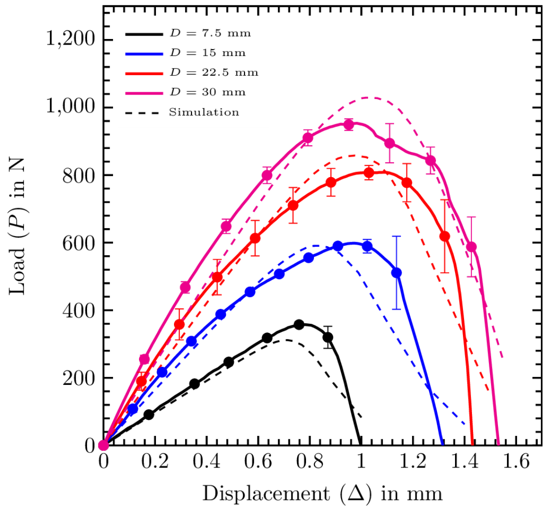

Figure 1.13: Comparison of Experimental and Numerical results

Table 1.8: Fracture Properties of DENT PC specimen by size effect law

Angle(θ)	G_f in kJ/m^2	c_f in mm
45	3.06	1.64
67	1.66	0.81
90	1.13	0.47

with thickness 2.1 mm. FE analysis is done for other thickness SENT and DENT specimen also. In all case, the overall load displacement repose matches very well with experiments. So traction separation curve derived from SEL is useful for numerical simulation of specimen with crack. Similar analysis have been done for Poly carbonate DENT specimen with different raster angle specimens.Poly carbonate fdm printed material shows the size effect law(SEL)for raster angle greater than 45^0 and which depends on raster angle of specimen Form the table, it can be seen that fracture energy decreases as raster angle of poly carbonate fdm material raster angle (θ) increases 1.8

1.9.2 Essential work of fracture analysis

The EWF concept originates fracture from the 70s from Broberg's unified theory of KB (1968)The total work of fracture includes both the dissipative work in the outer "plastic" zone and the essential one in the inner autonomous zone. The latter is called the fracture process zone, and the essential work of fracture represents a material property. the EWF technique was originally developed by B. Cotterell (1977). They have introduces the essential work of fracture for plane stress ductile fracture. The work perform at the tip of crack is called essential work of fracture and it is constant for a particular sheet thickness. They have performed experiment of a cold rolled low alloy steel in 16 gauge sheet for double edge notched tensile specimens in Mode-I. The total work of fracture (W_f) can be partitioned into two components; (i) the essential work of fracture (W_e) consumed in the inner fracture process zone to create new surface, and (ii) the non-essential (or plastic) work (W_p) performed in the outer "plastic" deformation zone see Figure 2.1. The total work of fracture (W_f), calculated from the area of the load–displacement curves is given by Eq. 1.5

$$W_f = W_e + W_p \tag{1.5}$$

Assuming that both zones are within the ligament of the specimen, Eq. 1.5 can be rewritten into the specific terms (Eq. 1.6 and 1.7)

$$W_f = w_e l B + \beta w_p l^2 w_p \tag{1.6}$$

$$w_f = w_e + \beta w_p l \tag{1.7}$$

Where l is the ligament length, B is the specimen thickness and β is the shape factor related to the form of the outer plastic dissipation zone. Accordingly w_e and w_p are surface and volume related, respectively. Eq. 1.7 provides the basis for data reduction: data on the specific work of fracture w_f determined on specimens with varying ligaments are plotted as a function of the ligament length l,such that w_e and w_p are given, respectively, by intercept on the w_f axis for $l = 0$, and the slope obtained by a the linear regression. The specific essential work increases

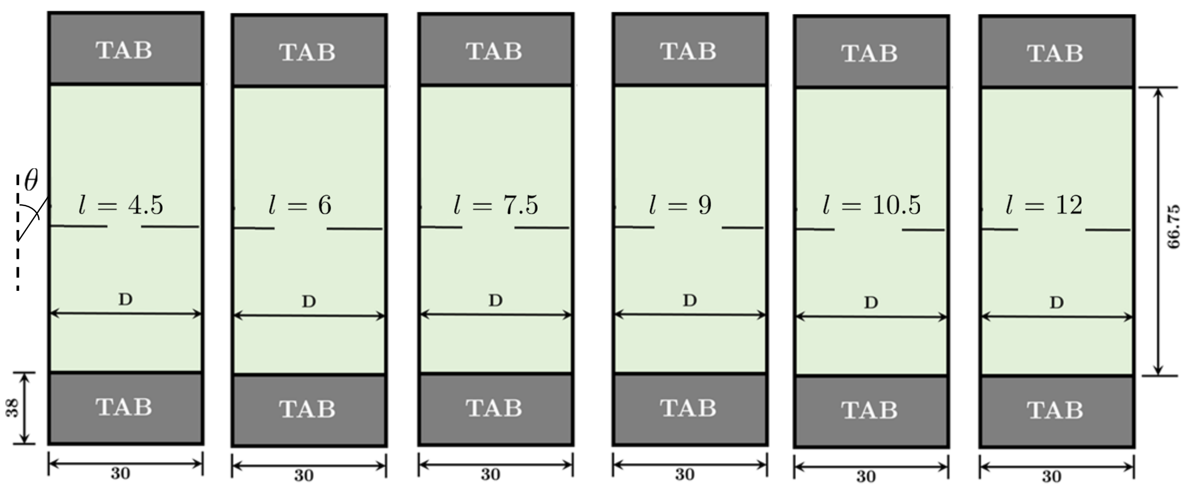

Figure 1.14: Schematic of DENT specimens for EWF

with sheet thickness. Fig. 1.14 shows the dimensions of the DENT specimen. These specimens were prepared using the FDM method with polycarbonate (PC)

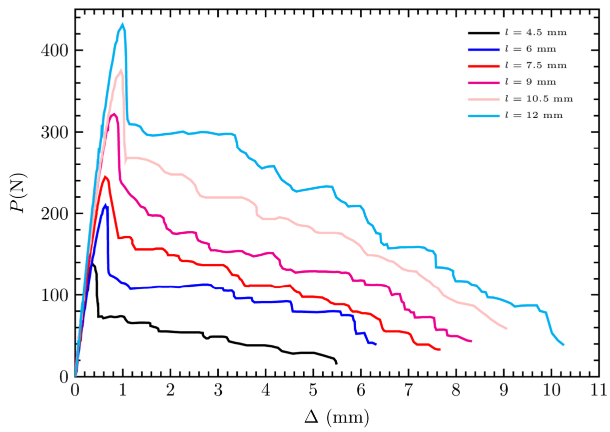

(a)

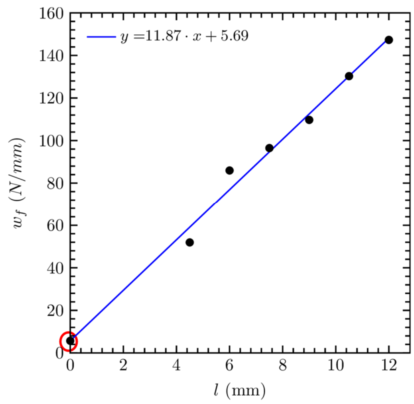

(b)

Figure 1.15: (a) P-Δ curve of Tested Specimens (b) EWF analysis of DENT specimen

material, employing a layer orientation of $[0/45/90/-45]$ and a layer height of 0.3 mm, resulting in a total specimen thickness of 1.2 mm. A crack with varying ligament lengths, according to the EWF approach described in Mai and Cotterell (1986), was created using a laser.

DENT specimens were tested on a UTM to extract load-displacement data, which is shown in Fig. 1.15 a. This data was then analyzed according to the EWF approach, where the area under the P-Δ curve was calculated for each ligament length. Subsequently, a graph of this area versus was plotted and extrapolated to zero ligament length to obtain the specific essential work of fracture as shown in fig. 1.15 b. Here D_L for all specimens are in the range of 0.15 to 1.5 so ductile behaviour is observed. Specific EWF (w_f) which fracture energy of specimen which is 5.69 kJ/m^2 for PC specimens. DENT specimens are tested on UTM for extraction of load-displacement data which is shown in fig.1.14. Then this data are analyzed as per EWF approach in area under P-Δ curve are calculated for each ligament length then this area versus graphs are plotted and extra to zero ligament length to get specific essential work of fracture

1.10 Conclusion

1. FDM printed carbon PLA laminate material test show that the nominal strength of laminate that are similar and have similar notches exhibits a size effect which depends on the specimen geometry as well as thickness. The size effect observed agree with SEL proposed by Bazant and Planas (1998), according to which the curve of nominal strength versus the strength the

size plot on logarithmic scale exhibits a smooth transition from ductile to LEFM type with increasing structure size. this behavior called as quasi brittle behavior.

2. Size effect tests can be used to determine the fracture characteristic of cracked carbon PLA laminate build with FDM process. This method is easier to implement than other methods due to peak load measurements are necessary. Fracture properties such as the fracture energy (G_f) and effective length of FPZ can be determined from size effect test. From results fracture energy of both SENT and DENT geometry are same but it depends on thickness. The size of FPZ length is different due to different geometry types. Crack resistance curve (R-curve) can also be determined from these characteristics for both SENT and DENT geometry. The shape of the R- curve also depends on the specimen thickness and geometry.

3. The fracture energy was numerically verified to check applicability of SEL. TSC was derived from SEL, and a numerical analysis was done using cohesive zone modeling technique. Good agreement was found between the G_f values derived by SEL and TSC. The numerical results also showed good agreement with experimental results. Therefore,TSC can be used for crack propagation analysis.

4. Poly carbonate (PC) FDM printed material shows the size effect law(SEL)for raster angle greater than 45^0 and which depends on raster angle of specimen.Fracture energy decreases as raster angle of poly carbonate FDM material raster angle (θ) increases.

5. The behavior of PC FDM-made laminate material, with one lamina having a 0^0 raster angle, shows ductile behavior. The EWF approach can be applied to PC FDM laminates to evaluate fracture toughness.

References

Ai J.R. and Vogt B.D. Size and print path effects on mechanical properties of material extrusion 3d printed plastics. *Progress in Additive Manufacturing*, 7: 1009–1021, 10 2022.

ASTM. ASTM D638 - 14 Standard Test Method for Tensile Properties of Plastics.

B. Cotterell J.K.R. The essential work of plane stress ductile fracture. . *International Journal of Fracture*, 13:267–77, 1977.

Bagsik A. and Manufacturing D. Mechanical Properties of Fused Deposition Modeling Pards with Ultem* 9085. *In Proceedings of the 14th International Scientific Conference on Polymeric Materials*, 15:307–315, 2011.

Bao G., Ho S., Suo Z., and Fan B. The role of material orthotropy in fracture specimens for composites. *International Journal of Solids and Structures*, 29(9): 1105–1116, 1992.

Bazant Z.P. Size Effect in Blunt Fracture: Concrete, Rock, Metal. *Journal of Engineering Mechanics*, 110(4):518–535, apr 1984.

Bazant Z.P. and Planas J. *Fracture and Size Effect in Concrete and other Quasibrittle Materials.* CRC Press, Boca Raton, 1998.

Bažant Z.P., Cedolin L., Chen W.F., and Lui E.M. Stability of Structures: Elastic, Inelastic, Fracture and Damage Theories . *Journal of Structural Engineering*, 119(3):1001–1002, mar 1993.

Bazant Z.P., Daniel I.M., and Li Z. Size Effect and Fracture Characteristics of Composite Laminates. *Journal of Engineering Materials and Technology*, 118 (3):317, jul 1996.

Casavola C., Cazzato A., Moramarco V., and Pappalettere C. Orthotropic mechanical properties of fused deposition modelling parts described by classical laminate theory. *Materials & Design*, 90:453–458, jan 2016.

Desai C.K., Basu S., and Parameswaran V. Determination of Traction Separation Law for Interfacial Failure in Adhesive Joints at Different Loading Rates. *The Journal of Adhesion*, 92(10):819–839, oct 2016.

Dugdale D.S. Yielding of steel sheets containing slits. *Journal of the Mechanics and Physics of Solids*, 8:100–104, 1960.

Garg A. and Bhattacharya A. An insight to the failure of FDM parts under tensile loading: finite element analysis and experimental study. *International Journal of Mechanical Sciences*, 120:225–236, jan 2017.

G.I. B. The formation of equilibrium cracks during brittle fracture.General ideas and hypothesis. Axisymmetrical cracks. *Journal of Applied Mathematics and Mechanics*, 23:622–636, 1959.

Hui C.Y., Xu D.B., and Kramer E.J. A fracture model for a weak interface in a viscoelastic material (small scale yielding analysis). *Journal of Applied Physics*, 72:3294–3304, 1992.

Ji S. and Guvendiren M. Recent Advances in Bioink Design for 3D Bioprinting of Tissues and Organs, 2017.

KB B. Critical review of some theories in fracture mechanics . *International Journal of Fracture*, 4(3):11–18, 1968.

Kobryn P.A., Ontko N.R., Perkins L.P., and Tiley J.S. Additive Manufacturing of Aerospace Alloys for Aircraft Structures, 2006.

Li H. and Chandra N. Analysis of crack growth and crack-tip plasticity in ductile materials using cohesive zone models. *International Journal of Plasticity*, 19: 849–882, 2003.

Li S., Thouless M.D., Waas A.M., Schroeder J.A., and Zavattieri P.D. Use of a cohesive-zone model to analyze the fracture of a fiber-reinforced polymer-matrix composite. *Composites Science and Technology*, 65(3-4):537–549, 2005.

Mai Y.G. and Cotterell B. On the essential work of ductile fracture in polymers. *International Journal of Fracture*, 32:105–125, 1986.

Martinez AB G.P.J. The essential work of fracture (EWF) method analyzing the post yielding fracture mechanics of polymers. . *Engineering Failure Analysis*, 16:2604–2617, 2009.

Maszybrocka J., Dworak M., Nowakowska G., Osak P., and Łosiewicz B. The influence of the gradient infill of pla samples produced with the fdm technique on their mechanical properties. *Materials*, 15, 2 2022.

Mohamed O.A., Masood S.H., and Bhowmik J.L. Mathematical modeling and FDM process parameters optimization using response surface methodology based on Q-optimal design. *Applied Mathematical Modelling*, 40(23-24):10052–10073, dec 2016.

Murr L.E. Frontiers of 3D Printing/Additive Manufacturing: from Human Organs to Aircraft Fabrication, 2016.

Needleman A. A continuum model for void nucleation by inclusion debonding. *Journal of Applied Mechanics*, 54:525–531, 1987.

Needleman A. An analysis of decohesion along an imperfect interface. *International Journal of Fracture*, 42:21–40, 1990a.

Panneerselvam T., Raghuraman S., and Krishnan N.V. Investigating mechanical properties of 3d-printed polyethylene terephthalate glycol material under fused deposition modeling. *Journal of The Institution of Engineers (India): Series C*, 102:375–387, 4 2021.

Pardoen T., Ferracin T., Landis C.M., and Delannay F. Constraint effects in adhesive joint fracture. *Journal of the Mechanics and Physics of Solids*, 53: 1951–1983, 2005.

Raut S., Jatti V.S., Khedkar N.K., and Singh T. Investigation of the Effect of Built Orientation on Mechanical Properties and Total Cost of FDM Parts. *Procedia Materials Science*, 6:1625–1630, 2014.

Rouf S., Raina A., Haq M.I.U., Naveed N., Jeganmohan S., and Kichloo A.F. 3d printed parts and mechanical properties: Influencing parameters, sustainability aspects, global market scenario, challenges and applications. *Advanced Industrial and Engineering Polymer Research*, 5:143–158, 7 2022.

Sagias V.D., Giannakopoulos K.I., and Stergiou C. Mechanical properties of 3d printed polymer specimens. *Procedia Structural Integrity*, 10:85–90, 1 2018.

Shet C. and Chandra N. Analysis of enerhy balance when using cohesive zone models to simulate fracture processes. *Journal of Engineering Materials and Technology*, 124:440–450, 2002.

Suresh S. Micromechanisms of fatigue crack growth retardation following overloads. *Engineering Fracture Mechanics*, 18(3):577–593, jan 1983.

Talagani F., DorMohammadi S., Dutton R., Godines C., Baid H., Abdi F., Kunc V., Compton B., Simunovic S., Duty C., Love L., Post B., and Blue C. Numerical simulation of big area additive manufacturing (3d printing) of a full size car. *Sampe Journal*, 51:27, 2015.

Tvergaard V. and Hutchinson J.W. The relation between crack growth resistance and fracture process parameters in elastic-plastic solids. *Journal of the Mechanics and Physics of Solids*, 40:1377–1397, 1992.

Wang X., Jiang M., Zhou Z., Gou J., and Hui D. 3D printing of polymer matrix composites: A review and prospective. *Composites Part B: Engineering*, 110: 442–458, feb 2017.

Wu W., Ye W., Wu Z., Geng P., Wang Y., and Zhao J. Influence of Layer Thickness, Raster Angle, Deformation Temperature and Recovery Temperature on the Shape-Memory Effect of 3D-Printed Polylactic Acid Samples. *Materials*, 10 (8):970, aug 2017.

Zhao Y., Chen Y., and Zhou Y. Novel mechanical models of tensile strength and elastic property of FDM AM PLA materials: Experimental and theoretical analyses. *Materials and Design*, 181:108089, 2019.

Zhu Y., Liechti K.M., and Ravi-Chandar K. Direct extraction of rate-dependent traction-separation laws for polyurea/steel interfaces. *International Journal of Solids and Structures*, 46(1):31–51, 2009.

Zou R., Xia Y., Liu S., Hu P., Hou W., Hu Q., and Shan C. Isotropic and anisotropic elasticity and yielding of 3D printed material. *Composites Part B: Engineering*, 99:506–513, aug 2016.